4th Micro and Nano Flows Conference
UCL, London, UK, 7-10 September 2014

Thermal Conductivity and Rheology Behavior of Aqueous Nanofluids Containing Alumina and Carbon Nanotubes

Zan WU [1,*], Zhaozan FENG [2], Lars WADSO [3], Bengt SUNDEN [1]

* Corresponding author: Tel.: +46 46 2228604; Fax: +46 46 2224717; Email: zan.wu@energy.lth.se
[1] Department of Energy Sciences, Lund University, Lund, Sweden
[2] Department of Energy Engineering, Zhejiang University, Hangzhou, China
[3] Division of Building Materials, Lund University, Lund, Sweden

Keywords: Nanofluid, Thermal conductivity, Viscosity, Carbon nanotube, Agglomeration, Interfacial thermal resistance

Abstract

In this study, thermal conductivity and rheology behavior of aqueous alumina and multi-walled carbon nanotube (MWCNT) nanofluids were measured and compared with several analytical models. Both thermal conductivity and viscosity of the two nanofluids increase with increasing volume fraction. The experimental thermal conductivity data for the two nanofluids are located near the lower Hashin-Shtrikman bound and far away from the upper Hashin-Shtrikman bound. Therefore there is still enough room for thermal conductivity enhancement. Further conductivity enhancement of the nanofluids can be achieved by manipulating particle or agglomeration distribution and morphology. The structure-property relationship was checked for the nanofluids. Possible agglomeration size and interfacial thermal resistance were obtained and partially validated. Based on the Chen et al. model, a revised model was developed by incorporating the effects of interfacial thermal resistance into the Hamilton-Crosser model. The revised model can accurately reproduce the experimental data based on the agglomeration size extracted from the rheology analysis. In addition, thermal conductivity change of the alumina/water nanofluid with elapsed time was also investigated. The average thermal conductivity decreases with elapsed time. Besides, thermal conductivity measurements were conducted for nanofluid mixtures of alumina/water and MWCNT/water nanofluids.

1. Introduction

Nanofluids are engineered colloidal suspensions of nanoparticles in a base fluid. They are more stable than microparticle colloids, with little particle setting, channel erosion and clogging. Nanofluids have distinctive features that offer potential for many applications in various fields including energy, bio and pharmaceutical processes, food industry, and chemical, electronic, environmental, material and thermal engineering etc. [1]. For example, nanofluids can be considered as a new class of heat-transfer fluids as they generally provide higher thermal conductivity compared to their based conventional heat-transfer fluids (e.g., water, ethylene glycol, engine oil). Various investigations [2-6] on nanofluids flowing in tubes and heat exchangers indicate that conventional pressure drop and heat transfer correlations for the base fluid can accurately reproduce the flow and thermal behaviors for nanofluids by adopting the measured nanofluid properties in the analysis, respectively. That means, the flow structure and the convective heat transfer mechanisms were probably not modified by the addition of nanoparticles. The benefit of using nanofluids for heat transfer improvement mainly comes from the thermal conductivity enhancement. The generally accompanied higher nanofluid viscosity requires a higher pumping power which may counterbalance the benefit of the enhanced thermal conductivity. Therefore, thermal conductivity and viscosity of nanofluids need to be investigated and manipulated for possible heat transfer and other relevant applications.

Thermal conductivity and viscosity of nanofluids are strongly dependent on particle concentration, particle size and shape, the presence of agglomerations (i.e., nanoclusters, aggregates), the nature of the base fluid, temperature and nanofluid stability. In nanofluids, nanoparticles tend to form agglomerations of different size due to the van der Waals attractive forces. Preparation methods such as addition of surfactants and ultrasonic vibration can reduce the size of the agglomerates substantially but are not able to break the agglomerates into primary particles. Existence of nanoparticle agglomerations has already been recognized by dynamic light scattering and SEM/TEM observations in the literature, e.g., [7-11]. Agglomeration tends to enhance nanofluid viscosity due to the immobilized fluid trapped in the particle clusters and thus a higher effective volume fraction than the actual solid volume fraction. Anoop et al. [7] considered the viscosity increase to be primarily due to the agglomeration of particles in water-based and ethylene-based nanofluids. With regard to thermal conductivity, there is still some controversy or discrepancy about the effects of agglomeration [8-11].

The lower and upper limits of the nanofluid thermal conductivity can be completely determined by the serial mode and the parallel mode [12] only using volume fractions and thermal conductivities of the two phases, respectively. Hashin and Shtrikman [13] proposed strict bounds based on the classical effective medium theory, which is given below for the case of $k_p/k_f > 1$

$$k_{\mathrm{f}}\left(1+\frac{3\varphi\left(k_{\mathrm{p}}-k_{\mathrm{f}}\right)}{3k_{\mathrm{f}}+\left(1-\varphi\right)\left(k_{\mathrm{p}}-k_{\mathrm{f}}\right)}\right)\leq k_{\mathrm{nf}}\leq k_{\mathrm{p}}\left(1-\frac{3\left(1-\varphi\right)\left(k_{\mathrm{p}}-k_{\mathrm{f}}\right)}{3k_{\mathrm{p}}-\varphi\left(k_{\mathrm{p}}-k_{\mathrm{f}}\right)}\right) \quad (1)$$

At the lower bound, nanoparticles are well-dispersed in the base fluid. At the upper bound, the nanoparticles form a continuous phase with linear or chainlike particle morphologies, and the base fluid becomes a dispersed phase. Besides the agglomeration morphology described above, liquid layering at the liquid-particle interface, Brownian motion and coupled transport can also influence the thermal conductivity located within the lower and upper bounds [14].

Mo et al. [15] observed the presence of an ordered liquid layer near a nanoparticle surface by which the atomic structure of the liquid near the surface is significantly more ordered than that of bulk liquid. The thermal conductivity of ordered liquid layers tends to be larger than that of the bulk base fluid. Therefore, ordered liquid layers may enhance the effective thermal conductivity of the nanofluid by augmenting the particle effective volume fraction. Wang and Fan [14] suggested the liquid layers offer insignificant conductivity enhancement for water-based nanofluids containing spherical particles as the liquid film thickness is only 0.28 nm for aqueous nanofluids. For nanoparticle size of the order of 10 nm, the increase in effective volume fraction induced by ordered liquid layers is only 0.1%, which contributes little. However, their presence may facilitate formation of interconnected particle agglomerations by relaxing the requirement of particle physical contact with each other. In addition, the liquid layering at the liquid-particle interface may present interfacial thermal resistance at the particle-fluid interface and among the particle-particle interface due to different nature of thermal conduction in nanoparticles and the base fluid, and thus decrease thermal conductivity enhancement.

Brownian motion can enable direct inter-particle transport of heat from one particle to another and induce surrounding fluid flow and thus so-called micro-convection. The ratio of the contribution to thermal conductivity by Brownian motion and micro-convection (k_{BM}) to the base fluid conductivity (k_{f}) was estimated based on the kinetic theory by Evans et al. [16]

$$\frac{k_{\mathrm{BM}}}{k_{\mathrm{f}}}=\frac{\rho_{\mathrm{p}}c_{\mathrm{p,f}}\varphi k_{\mathrm{B}}T}{3\pi\mu_{\mathrm{f}}d_{\mathrm{p}}k_{\mathrm{f}}}+\frac{k_{\mathrm{B}}T}{3\pi\mu_{\mathrm{f}}d_{\mathrm{p}}\alpha_{\mathrm{f}}} \quad (2)$$

According to the above equation, the contribution of Brownian motion and micro-convection for nanofluids can be negligible in our case, as stated in [16-18].

Eapen et al. [18] believed that both the Soret effect (also known as thermodiffusion or thermophoresis) and the Dufour effect (an induced heat flow caused by the concentration gradient) do not directly influence the nanofluid thermal conductivity by analyzing the orders of magnitude, but the coupled or crossed transport between them or other transport processes might affect the thermal conductivity. As proposed in Ref. [14], the coupled transport could change the nature of heat conduction in nanofluids from a diffusion process to a wave process, thus giving a nanofluid thermal conductivity enhancement as high as 10%.

Based on the above statement, more experimental data are needed to better understand the nanoparticle behavior and identify possible underlying mechanisms for thermal conductivity enhancement in various nanofluids. The purpose of this study is to measure the thermal conductivity and viscosity of aqueous alumina and aqueous multi-walled carbon nanotube (MWCNT) nanofluids of different volume fractions, and to examine various analytical thermal conductivity and viscosity models to explain the possible related mechanisms in our tested nanofluids. For example, effects of particle agglomeration morphology and possible interfacial thermal resistance will be recognized and analyzed. In addition, thermal conductivity values of mixture of alumina/water nanofluid and MWCNT/water nanofluid will also be measured for the first time.

2. Results and Discussion

2.1 Alumina nanofluid

Untreated concentrated γ-Al_2O_3/water nanofluid with spherical alumina nanoparticles of 40-nm mean diameter was purchased from a commercial company (Nanophase Technologies Corporation, US). No surfactants were added in the nanofluid. Different amounts of concentrated nanofluid were diluted in water to obtain nanofluids with different concentrations. The diluted nanofluid mixture was mechanically stirred for 0.5 h followed by ultrasonic vibration for 3 h. Nine nanofluids with particle volume fractions, 1.0%, 1.51%, 1.89%, 2.99%, 4.99%, 6.0%, 7.82%, 9.84% and 18.4% were carefully prepared. For aqueous nanofluids, pH control, which has an important role in stability control, places the iso-electric point, far from the point of zero charge in order to avoid coagulation and instability. The pH value of the prepared alumina nanofluid is about 3 ~ 3.5, which is far away from the iso-electric point of alumina nanofluid.

A thermal constants analyzer (TPS 2500S from Hot Disk AB, Sweden) using the transient plane source method (TPS) was employed to measure the thermal conductivity of aqueous alumina and MWCNT nanofluids. The diameter of the used Hot Disk sensor is 2.0 mm. For each test, the measurement time and the total output of power were limited to 2 seconds and 0.015 W, respectively. Therefore, natural convection can be ignored due to the low temperature rise of the sensor. Before nanofluid measurements, several pure fluids were tested to check the accuracy of the TPS method. The thermal conductivity values of these pure fluids are listed in Table 1. The thermal conductivity uncertainty was estimated, from the standard deviations of experimental data and departures from literature data, to be lower than 3.0 %.

Table 1 Experimental thermal conductivity for pure fluids at 20 °C.

Material	k (W m^{-1} K^{-1})	Material	k (W m^{-1} K^{-1})
Water	0.583	Ethylene glycol	0.244
Ethanol	0.1695	Glycerol	0.272
1-Butanol	0.1515	2-Propanal	0.1395
Olive oil	0.1691		

A rotational rheometer HAAKE RS6000 (Thermo Fisher Scientific Inc., US) was used to measure rheology behavior of alumina/water and MWCNT/water nanofluids. The standard deviation of the measured dynamic viscosity data of water (the base fluid) and departures from the literature data is less than 3.0%.

Figure 1 shows the relative thermal conductivity k_{nf}/k_f of alumina/water nanofluids of different volume fractions. The thermal conductivity increases with volume fraction. Previous data of Williams et al. [19] and Timofeeva et al. [20] were also shown for comparison. All the data sets give similar trends, especially at low volume fractions. The present data is higher than that of Timofeeva et al. [20] when the volume fraction is larger than 0.03, while lower than that of Williams et al. [19] when the volume fraction is between 0.01 and 0.05. Overall, the difference among the three data sets at the same volume fraction is less than 10%.

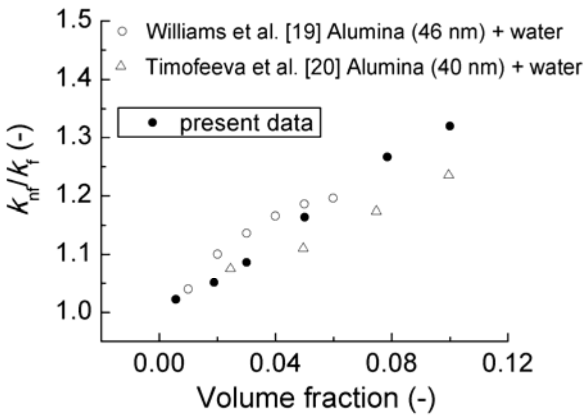

Fig. 1 Relative thermal conductivity of alumina/water nanofluid versus volume fraction at 20 °C.

Figure 2 presents the evaluation of the present data and several analytic models. The present data points are almost located within the lower and upper H-S bounds. The lower H-S bound or the Maxwell model can estimate the present data decently, especially at volume fractions lower than 3.0%. The Bruggeman model (BGM) [21] can predict the data well except those with volume fractions larger than 8%.

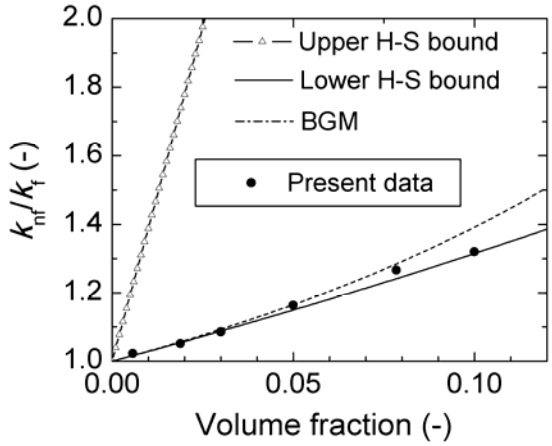

Fig. 2 Evaluation of the lower and upper H-S bounds [13] and the Bruggeman model (BGM) [21] by the present data for alumina/water nanofluid.

Measurements of the change of alumina/water nanofluid thermal conductivity with elapsed time were also performed at static conditions, as shown in Fig. 3. The alumina/water nanofluid has a volume fraction of 7.82%. In general, thermal conductivity decreases with elapsed time. A 7.0% reduction in thermal conductivity averaged for each day can be seen in Fig. 3 after 55 days. Possible reasons for thermal conductivity reduction are the formation of relatively large nanoparticle clusters and deposition. More experimental investigations are needed to better understand this phenomenon.

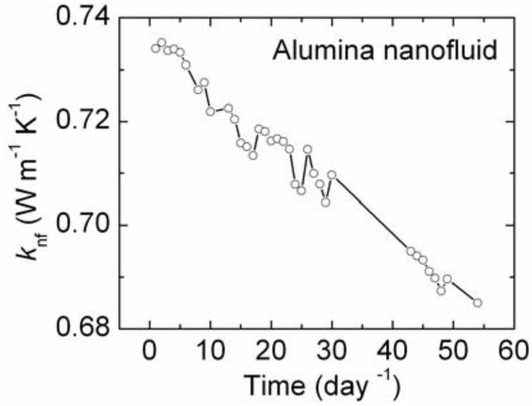

Fig. 3 The change of thermal conductivity averaged for each day with elapsed time for alumina/water nanofluid at 20 °C.

Rheology behavior of the alumina/water nanofluid is demonstrated in Fig. 4 for those data points with shear rates larger than 30 s^{-1}. The dynamic viscosity seems to be almost constant for the tested shear rates. Alumina nanofluids of high volume fractions may present non-Newtonian behavior, especially at very low shear rates. In our case, however, it is hard to see obvious non-Newtonian behavior for volume fractions up to 18.4% when the shear rate is larger than 50 s^{-1}. Therefore, the tested nanofluids can be regarded as Newtonian fluids when the shear rate is larger than 50 s^{-1}.

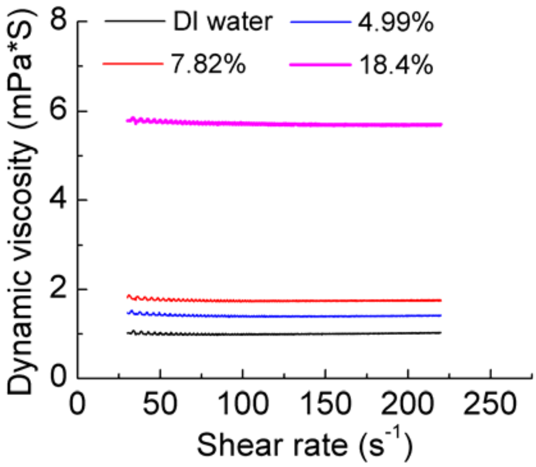

Fig. 4 Rheology behavior of alumina/water nanofluids at 20 °C.

Figure 5 shows the relative dynamic viscosity μ_{nf}/μ_f of alumina/water nanofluids versus volume fraction. For the present data, the measured dynamic viscosity values at a shear rate of 210 s^{-1} were used. The relative dynamic viscosity increases with volume fraction. The increase rate seems to become higher at larger volume fractions. Previous literature data of Anoop et al. [7], Williams et al. [19] and Sahoo et al. [22] are also shown for comparison. The viscosity data of Anoop et al. [7], Sahoo et al. [22] and the present alumina viscosity data show very similar trends. The viscosity data of Williams et al. [19] is much higher than that of the other three data sets. Therefore, the present tested alumina nanofluid seems to give better convective heat transfer performance than that of Williams et al. [19] as it has a decent thermal conductivity enhancement but relatively low viscosity enhancement.

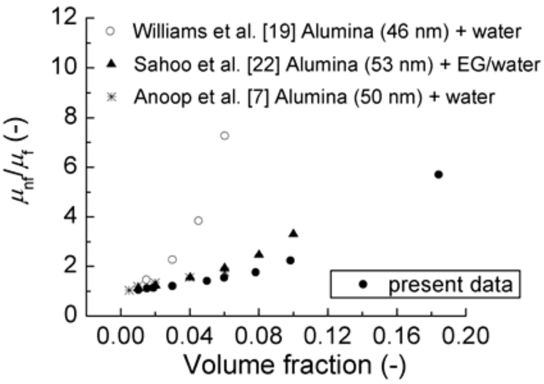

Fig. 5 Relative dynamic viscosity of alumina/water nanofluid versus volume fraction at 20 °C.

Comparison of the present data with that predicted by the Batchelor model [23] and the Chen et al. model [24] is shown in Fig. 6. Chen et al. [24] proposed to calculate the effective dynamic viscosity by integrating the aggregation mechanism into the Krieger and Dougherty [25] model. Please refer to Chen et al. [24] for detailed equations. Different agglomeration sizes were used in the Chen et al. model to guess the agglomeration size of the tested alumina/water nanofluid. The statement $d_a = d_p$ means no agglomeration. As can be seen in Fig. 6, both the Batchelor model and the Chen et al. model of no agglomeration under-predict the dynamic viscosity, especially at relatively high volume fractions. The Chen et al. model can accurately reproduce the present data for volume fractions less than about 15% when $d_a = 2.16\ d_p$. That means, nanoparticles might agglomerate in our tested alumina/water nanofluid and the agglomeration size is about 2.16 times of the particle diameter. We further verified the agglomeration size through dynamic light scattering (DLS) measurements. Nanofluids of three different volume fractions, i.e., 1.0%, 1.89% and 4.99% were observed by DLS. Nanofluids were diluted carefully for DLS measurements. The three nanofluids give similar particle size distributions and have a peak at 80-95 nm, which confirmed the agglomeration size. For an agglomeration size of 2.16 d_p, three nanoparticles might agglomerate and closely packed together, with a small amount of liquid trapped in the agglomeration core.

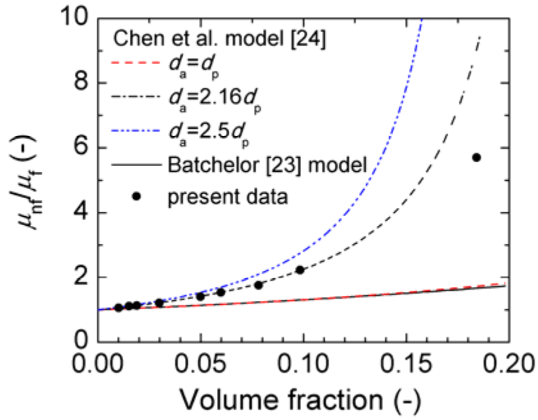

Fig. 6 Comparison of the present data with that predicted by the Batchelor model [23] and the Chen et al. model [24].

According to the discussion by Chen et al. [26], the effective thermal conductivity can be predicted based on the rheology analysis by including particle agglomeration. As the approximate agglomeration size of the tested nanofluids has been extracted from Fig. 6, we can check if the measured thermal conductivity can be predicted by taking the effect of agglomeration into account. The blue dotted line in Fig. 7 without interfacial thermal resistance is the Chen et al. model [26]. The Chen et al. model over-estimates the present data largely. Therefore, an interfacial thermal resistance may exist within the agglomerate and at the liquid/solid interfaces. We revised the Chen et al. model by incorporating the effects of interfacial thermal resistance. The revised model is shown as follows

$$\frac{k_{nf}}{k_f}=\frac{k_a(1+2\cdot \mathrm{Bi})+(n-1)k_f+(n-1)\varphi_a\left[k_a(1-\mathrm{Bi})-k_f\right]}{k_a(1+2\cdot \mathrm{Bi})+(n-1)k_f-\varphi_a\left(k_a(1-\mathrm{Bi})-k_f\right)} \quad (3)$$

where Bi is the particle Biot number defined as $2R_k k_f/d_a$. As shown in Fig. 7, the revised model can reproduce our thermal conductivity data by using an interfacial thermal resistance R_k of 1.9×10^{-8} m^2 K W^{-1}. Thus, we can conclude that the tested alumina nanofluid in this study contains agglomerations of an approximate size of 2.16 d_p, and an interfacial thermal resistance, which degrades thermal conductivity, exists in our case and can not be neglected.

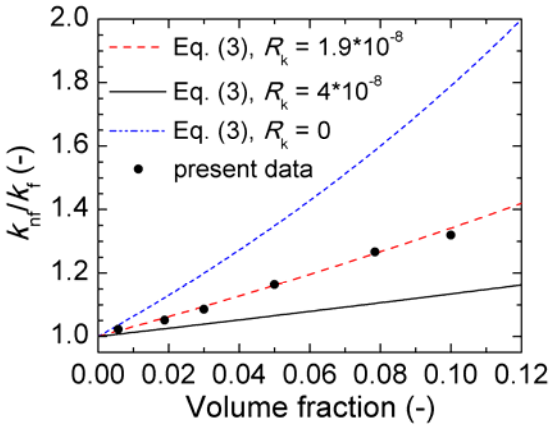

Fig. 7 Evaluation of the revised model based on Chen et al. [26] at different values of interfacial thermal resistance for alumina/water nanofluid.

2.2 MWCNT/water nanofluid

An aqueous MWCNT suspension of 1.0% mass fraction was purchased from a commercial company (Nanocyl, Belgium). According to the vendor's specification, the suspension consists of thin MWCNTs dispersed in de-ionized (DI) water (97% mass fraction) and surfactant sodium dodecyl benzene sulfonate (SDBS, 2.0% mass fraction), and it is said to be stable for several months. The MWCNT, produced via the catalytic carbon vapor deposition (CCVD) process, has an average length of 1.5 μm and an average diameter of 9.5 nm, with an average aspect ratio of 158. The surface area of the MWCNT is 250-300 m^2/g. The carbon purity of the MWCNTs is 90%, while the remaining 10% is metal oxide. Similar to alumina nanofluid, different amounts of concentrated nanofluid were diluted in water to obtain MWCNT/water nanofluids with different concentrations. The diluted nanofluid mixture was mechanically stirred for 0.5 h followed by ultrasonic vibration for 3 h. Four MWCNT/water nanofluids with carbon nanotube (CNT) volume fractions, 0.0278%, 0.0555%, 0.278% and 0.557% were carefully prepared. The pH values of the prepared MWCNT/water nanofluids are in the range 7.0 ~ 8.0.

Figure 8 shows the relative thermal conductivity k_{nf}/k_f of MWCNT/water nanofluids of different volume fractions. Basically, the thermal conductivity increases with volume fraction. Literature data of Cherkasova and Shan [27], Meng et al. [28], Ding et al. [29] and Phuoc et al. [30] are also shown in Fig. 8 for comparison. The present relative thermal conductivity and the data of Meng et al. [28] and Phuoc et al. [30] give similar values and trends. The data sets of Cherkasova and Shan [27] and Ding et al. [29] are higher than the other three data sets and suggest that MWCNT/water nanofluids, if prepared properly, can provide decent thermal conductivity enhancements even at very low volume fractions.

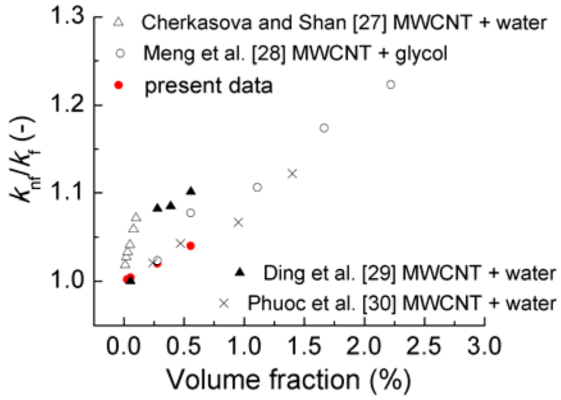

Fig. 8 Relative thermal conductivity of MWCNT/water nanofluid versus volume fraction at 20 °C.

As CNTs of large aspect ratio tend to bend very easily, a non-straightness parameter η can be used to represent the aggregated or entangled state of the CNTs, which is described as:

$$\eta = \frac{L_{\mathrm{actual}}}{L_{\mathrm{p}}} \tag{4}$$

where L_{actual} is the distance between the two ends of the non-straight CNT. Deng et al. [31] developed a thermal conductivity model by adopting the non-straightness parameter. Figure 9 demonstrates the Deng et al. model at four different volume fractions. The relative thermal conductivity increases with volume fraction and non-straightness factor. The relative thermal conductivity increases with non-straightness factor very quickly when the non-straightness of CNTs is low, i.e., severe entanglement, and then gradually saturates. Therefore, methods should be figured out to avoid severe CNT entanglements and aggregations for thermal conductivity enhancement. As shown in Fig. 9, the non-straightness factor in our MWCNT/water nanofluids is in the range 0.11-0.13, indicating relatively severe CNT entanglement. This is a possible reason for the relatively low thermal conductivity of the tested MWCNT/water nanofluid.

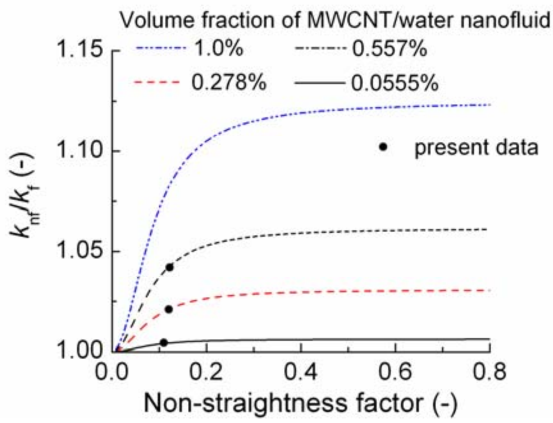

Fig. 9 Comparison of the Deng et al. model [31] with the present data for MWCNT/water nanofluid.

Rheology behavior of MWCNT/water nanofluids with volume fractions of 0.0278% and 0.557% is demonstrated in Fig. 10. The horizontal solid line in Fig. 10 indicates the dynamic viscosity value for water at 20 °C. The 0.557% nanofluid behaves as a shear-thinning fluid (non-Newtonian fluid) as the dynamic viscosity decreases when the shear rate increases, especially at low shear rates. When the shear rate is larger than 150 s^{-1}, the viscosity is independent of the shear rate. The 0.0278% nanofluid behaves like a Newtonian fluid, at least for shear rates larger than 50 s^{-1}.

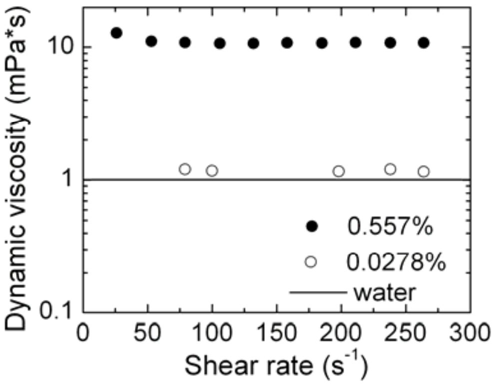

Fig. 10 Rheology behavior of MWCNT/water nanofluids at 20 °C.

Figure 11 shows the relative viscosity of the present MWCNT/water data and that of Phuoc et al. [30] and Halelfadl et al. [32]. For the present data, measured viscosities at a high shear rate of 264 s^{-1} were used. The relative viscosity increases with volume fraction. The increase rate also increases with volume fraction for the present data and the data of Halelfadl et al. [32]. The data of Phuoc et al. [30] is much lower than the present data and that of Halelfadl et al. [32].

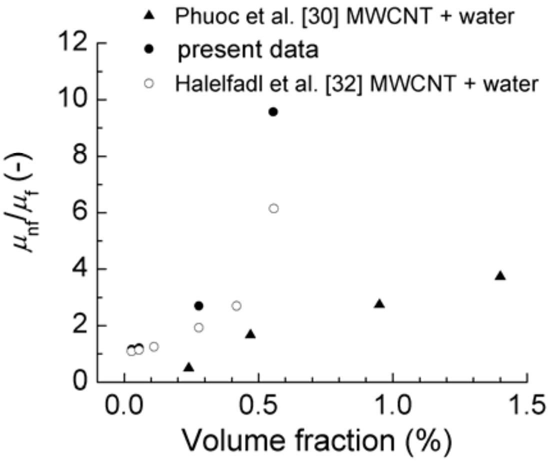

Fig. 11. The relative viscosity of MWCNT/water nanofluids versus volume fraction at 20 °C.

Comparison of the present data with that predicted by the Halelfadl et al. model [32] of different agglomeration sizes is shown in Fig. 12. The present data can be predicted well when $d_a = 5.6\ d_p$.

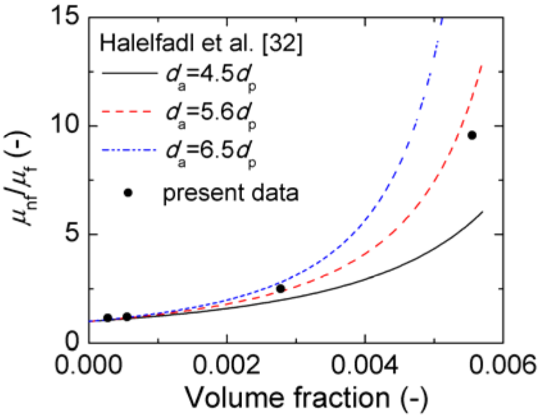

Fig. 12 Comparison of the present data with that predicted by the Halelfadl et al. model [32] for MWCNT/water nanofluid.

Based on the above analysis, the MWCNTs in the tested nanofluid are entangled and agglomerated in the base fluid. According to DLS observation, the particle size distributions of the tested nanofluids have peak values located within 190-230 nm. The non-straightness factor is in the range 0.11-0.13 as shown in Fig. 9, which corresponds to L_{actual} values from 165 to 195 nm. If we define L_{actual} as the distance between the two ends of an agglomeration or aggregation rather than the two ends of a non-straight CNT, the value from DLS observation and that obtained from the Deng et al. model [31] are of the same order of magnitude. In this study, we assume that the MWCNT agglomeration is in the form of rod-like particles with a diameter of about 5.6 d_p (53 nm) and a length of about 200 nm, thus with an aspect ratio of 3.8. Therefore we can check if the revised model based on Chen et al. [26] can reproduce the thermal conductivity. During the calculation, thermal conductivities of carbon nanotubes along transverse and longitudinal directions and isotropic thermal conductivity of the nanotube are 5.6 W m^{-1} K^{-1}, 3000 W m^{-1} K^{-1} [33] and 2000 W m^{-1} K^{-1}, respectively. As shown in Fig. 13, the revised model can reproduce our thermal conductivity data by using an interfacial thermal resistance R_k of 1.2×10^{-8} m^2 K W^{-1}. Thus, the tested MWCNT nanofluid in this study contains agglomerations, and an interfacial thermal resistance, which degrades thermal conductivity, probably exists in our case and can not be neglected.

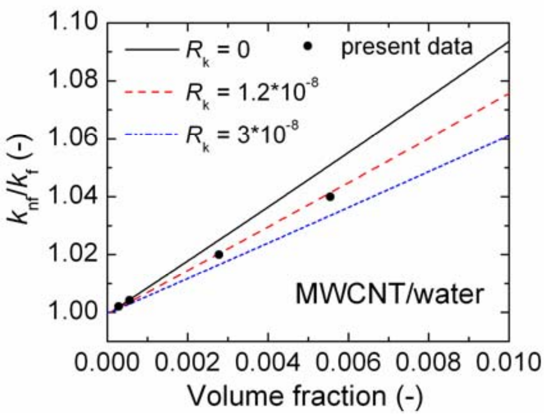

Fig. 13 Evaluation of the revised model at different values of interfacial thermal resistance for MWCNT/water nanofluid.

2.3 Nanofluid mixtures of alumina/water and MWCNT/water nanofluids

Two mixture samples listed in Table 2 of different alumina volume fractions were obtained and ultrasonically vibrated for 3 hours. The measured thermal conductivity values of the mixture are also listed in Table 2. The two samples have different alumina nanoparticle volume fractions.

Table 2 Thermal conductivity of two nanofluid mixtures.

Sample	Mixture contents	k_{nf} ($Wm^{-1}K^{-1}$)	k_{nf}/k_f (-)
No. 1	MWCNT/water 0.278% 10 mL Alumina/water 1.89% 25 mL	0.625	1.072
No. 2	MWCNT/water 0.278% 10 mL Alumina/water 5.0% 25 mL	0.629	1.079

As shown in Table 2, the thermal conductivity enhancement for sample No. 1 is 7.2%, which is slightly larger than the addition of that of the two original nanofluids. One possible reason might be that the agglomerate morphology has been modified. For sample No. 2, the thermal conductivity enhancement of 7.9% is less than the addition of that of the two original nanofluids. The thermal conductivity enhancement of sample No. 2 is almost the same as sample No. 1. An obvious increase in the alumina volume fraction for No. 2 does not produce an obvious enhancement, which is probably due to large interfacial thermal resistances and cluster deposition.

3. Conclusions

Thermal conductivity and rheology behavior of aqueous alumina and MWCNT nanofluids were measured and compared with several analytical models. Thermal conductivity and viscosity increase with increasing volume fraction. The tested alumina nanofluid may give a good convective heat transfer performance as it has a decent thermal conductivity enhancement and relatively low viscosity enhancement compared to literature data, while the tested MWCNT/water nanofluid is not efficient for convective heat transfer due to its large viscosity enhancement and relatively low thermal conductivity enhancement. The measured thermal conductivity values for both nanofluids are located near the lower H-S bound and far away from the upper H-S bound. Thus there is still room for thermal conductivity enhancement. Further conductivity enhancement can be achieved by manipulating particle or agglomeration distribution and morphology in the nanofluid. The structure-property relationship was exemplified in this study. Information about possible agglomeration size and interfacial thermal resistance were obtained and partially validated. SEM/TEM observations are required for further validation. By incorporating the effects of interfacial thermal resistance into the Chen et al. model, the revised model can reproduce the experimental data well based on the agglomeration size extracted from the rheology analysis.

The change of the thermal conductivity of alumina/water nanofluid with elapsed time was also investigated. A 7.0% reduction in average thermal conductivity was observed after 55 days. Possible reasons for the thermal conductivity reduction might be the formation of relatively large nanoparticle clusters and deposition. More experimental investigations are needed to better understand the change of thermal conductivity with time.

Besides, thermal conductivity measurements were conducted for nanofluid mixtures of alumina/water and MWCNT/water nanofluids. Proper proportions of the two nanofluids may give high thermal conductivity enhancement which is larger than the addition of that of the two original nanofluids by modifying agglomeration morphology. The obvious increase in the alumina volume fraction for sample No. 2 does not produce an obvious enhancement, which is probably due to large interfacial thermal resistances and cluster deposition.

Acknowledgements

Financial support from the Swedish Energy Agency and the Swedish Research Council (VR) are gratefully acknowledged. Special thanks to Prof. W. Li at Zhejiang University for his help on viscosity measurement of nanofluids.

Nomenclature

Bi	particle Biot number
$c_{p,f}$	specific heat at constant pressure (J kg^{-1} K^{-1})
d_a	agglomerate diameter (m)
d_p	particle diameter (m)
k	thermal conductivity (W m^{-1} K^{-1})
k_B	Boltzmann constant (m^2 kg s^{-2} K^{-1})
L_p	length of the particle (m)
n	shape factor
R_k	interfacial thermal resistance (m^2 K W^{-1})
Greek symbols	
η	non-straightness factor
μ	dynamic viscosity (Pa s)
ρ	density (kg m^{-3})
φ	volume fraction
Subscripts	
a	agglomeration
f	base fluid
nf	nanofluid
p	nanoparticles

References

[1] Wang, L., Fan, J. (2010). Nanofluids research: key issues. Nanoscale Res. Lett., 5(8), 1241-1252.
[2] Yu, W., France, D. M., Timofeeva, E. V., Singh, D., Routbort, J. L., Dakota, S. (2011). Convective heat transfer of nanofluids in turbulent flow. In: Carbon Nano Materials and Applications Workshop, Oct. 30-Nov. 1, South Dakota.
[3] Wu, Z., Wang, L., Sundén, B. (2013). Pressure drop and convective heat transfer of water and nanofluids in a double-pipe helical heat exchanger. Appl. Therm. Eng., 60(1), 266-274.
[4] Wu, Z., Wang, L., Sundén, B. (2013). Convective heat transfer of alumina/water nanofluids in a double-pipe helical

heat exchanger, 8th International Conference on Multiphase Flow ICMF 13, Jeju, Korea, May 26-31, 2013.

[5] Feng, Z. Z., Li, W. (2013). Laminar mixed convection of large-Prandtl-number in-tube nanofluid flow, Part I: Experimental study. Int. J. Heat Mass Transfer, 65, 919-927.

[6] Haghighi, E. B., Saleemi, M., Nikkam, N., Khodabandeh, R., Toprak, M. S., Muhammed, M., Palm, B. (2014). Accurate basis of comparison for convective heat transfer in nanofluids. Int. Commu. Heat Mass Transfer, 52, 1-7.

[7] Anoop, K. B., Kabelac, S., Sundararajan, T., Das, S. K. (2009). Rheological and flow characteristics of nanofluids: Influence of electroviscous effects and particle agglomeration. J. Appl. Phys., 106(3), 034909.

[8] Hong, K. S., Hong, T. K., Yang, H. S. (2006). Thermal conductivity of Fe nanofluids depending on the cluster size of nanoparticles. Appl. Phys. Lett., 88(3), 031901.

[9] Karthikeyan, N. R., Philip, J., Raj, B. (2008). Effect of clustering on the thermal conductivity of nanofluids. Mater. Chem. Phys., 109(1), 50-55.

[10] Keblinski, P., Phillpot, S. R., Choi, S. U. S., & Eastman, J. A. (2002). Mechanisms of heat flow in suspensions of nano-sized particles (nanofluids). Int. J. Heat Mass Transfer, 45(4), 855-863.

[11] Prasher, R., Phelan, P. E., Bhattacharya, P. (2006). Effect of aggregation kinetics on the thermal conductivity of nanoscale colloidal solutions (nanofluid). Nano Lett., 6(7), 1529-1534.

[12] Nielsen, L.E. (1978). Predicting the Properties of Mixtures: Mixture Rules in Science and Engineering, Dekker, New York.

[13] Hashin, Z., Shtrikman, S. (1963). A variational approach to the theory of the elastic behaviour of multiphase materials. J. Mech. Phys. Solids, 11(2), 127-140.

[14] Wang, L., Fan, J. (2011). Toward nanofluids of ultra-high thermal conductivity. Nanoscale Res. Lett., 6(1), 1-9.

[15] Mo, H., Evmenenko, G., Dutta, P. (2005). Ordering of liquid squalane near a solid surface. Chem. Phys. Lett., 415(1), 106-109.

[16] Evans, W., Fish, J., Keblinski, P. (2006). Role of Brownian motion hydrodynamics on nanofluid thermal conductivity. Appl. Phys. Lett., 88(9), 093116.

[17] Buongiorno, J. (2006). Convective transport in nanofluids. J. Heat Transfer, 128(3), 240-250.

[18] Eapen, J., Rusconi, R., Piazza, R., Yip, S. (2010). The classical nature of thermal conduction in nanofluids. J. Heat Transfer, 132(10), 102402.

[19] Williams, W., Hu, L. W., Buongiorno, J. (2008). Experimental investigation of turbulent convective heat transfer and pressure loss of alumina/water and zirconia/water nanoparticle colloids (nanofluids) in horizontal tubes. J. Heat Transfer, 130(4), 042412.

[20] Timofeeva, E. V., Gavrilov, A. N., McCloskey, J. M., Tolmachev, Y. V., Sprunt, S., Lopatina, L. M., Selinger, J. V. (2007). Thermal conductivity and particle agglomeration in alumina nanofluids: experiment and theory. Phys. Rev. E, 76(6), 061203.

[21] Bruggeman, D. A. G. (1935). Dielectric constant and conductivity of mixtures of isotropic materials. Ann. Phys. (Leipzig), 24, 636-679.

[22] Sahoo, B. C., Vajjha, R. S., Ganguli, R., Chukwu, G. A., Das, D. K. (2009). Determination of rheological behavior of aluminum oxide nanofluid and development of new viscosity correlations. Petroleum Sci. Tech., 27(15), 1757-1770.

[23] Batchelor, G. K. (1977). The effect of Brownian motion on the bulk stress in a suspension of spherical particles. J. Fluid Mech., 83(01), 97-117.

[24] Chen, H., Ding, Y., Tan, C. (2007). Rheological behaviour of nanofluids. New J. Phys., 9(10), 367.

[25] Krieger, I. M., Dougherty, T. J. (1959). Concentration dependence of the viscosity of suspensions. Trans. Soc. Rheol, 3, 137-152.

[26] Chen, H., Witharana, S., Jin, Y., Kim, C., Ding, Y. (2009). Predicting thermal conductivity of liquid suspensions of nanoparticles (nanofluids) based on rheology. Particuology, 7(2), 151-157.

[27] Cherkasova, A. S., Shan, J. W. (2010). Particle aspect-ratio and agglomeration-state effects on the effective thermal conductivity of aqueous suspensions of multiwalled carbon nanotubes. J. Heat Transfer, 132(8), 082402.

[28] Meng, Z., Wu, D., Wang, L., Zhu, H., Li, Q. (2012). Carbon nanotube glycol nanofluids: Photo-thermal properties, thermal conductivities and rheological behavior. Particuology, 10(5), 614-618.

[29] Ding, Y., Alias, H., Wen, D., Williams, R. A. (2006). Heat transfer of aqueous suspensions of carbon nanotubes (CNT nanofluids). Int. J. Heat Mass Transfer, 49(1), 240-250.

[30] Phuoc, T. X., Massoudi, M., Chen, R. H. (2011). Viscosity and thermal conductivity of nanofluids containing multi-walled carbon nanotubes stabilized by chitosan. Int. J. Therm. Sci., 50(1), 12-18.

[31] Deng, F., Zheng, Q. S., Wang, L. F., Nan, C. W. (2007). Effects of anisotropy, aspect ratio, and nonstraightness of carbon nanotubes on thermal conductivity of carbon nanotube composites. Appl. Phys. Lett., 90(2), 021914.

[32] Halelfadl, S., Estelle, P., Aladag, B., Doner, N., Mare, T. (2013). Viscosity of carbon nanotubes water based nanofluids: Influence of concentration and temperature, Int. J. Therm. Sci. 71, 111-117.

[33] Che, J., Cagin, T., Goddard III, W. A. (2000). Thermal conductivity of carbon nanotubes. Nanotechnology, 11(2), 65.